
# Absence of ferromagnetic order in high quality bulk Co-doped ZnO samples

H. B. de Carvalho, M. P. F. de Godoy, R. W. D. Paes, M. Mir, A. Ortiz de Zevallos et al.

Citation: J. Appl. Phys. **108**, 033914 (2010); doi: 10.1063/1.3459885

View online: http://dx.doi.org/10.1063/1.3459885

View Table of Contents: http://jap.aip.org/resource/1/JAPIAU/v108/i3

Published by the American Institute of Physics.

# Absence of ferromagnetic order in high quality bulk Co-doped ZnO samples

H. B. de Carvalho,[1,a)] M. P. F. de Godoy,[2] R. W. D. Paes,[3] M. Mir,[1] A. Ortiz de Zevallos,[4] F. Iikawa,[4] M. J. S. P. Brasil,[4] V. A. Chitta,[5] W. B. Ferraz,[6] M. A. Boselli,[3] and A. C. S. Sabioni[3]

[1]*Universidade Federal de Alfenas, 37130-000 Alfenas, Minas Gerais, Brazil*
[2]*Universidade Federal do ABC, 09210-170 Santo André, Sao Paulo, Brazil*
[3]*Universidade Federal de Ouro Preto, 35400-000 Ouro Preto, Minas Gerais, Brazil*
[4]*Instituto de Física Gleb Wataghin, Universidade Estadual de Campinas, 13083-970 Campinas, Sao Paulo, Brazil*
[5]*Instituto de Física, Universidade de São Paulo, P.O. Box 66318, 05315-970 São Paulo, Sao Paulo, Brazil*
[6]*Centro de Desenvolvimento de Tecnologia Nuclear/CNEN, 31270-901 Belo Horizonte, Minas Gerais, Brazil*

(Received 29 April 2010; accepted 3 June 2010; published online 11 August 2010; corrected 16 August 2010)

Bulk $Zn_{1-x}Co_xO$ samples were synthesized via standard solid-state reaction route with different Co molar concentrations up to 21%. A detailed microstructural analysis was carried out to investigate alternative sources of ferromagnetism, such as secondary phases and nanocrystals embedded in the bulk material. Conjugating different techniques we confirmed the Zn replacement by Co ions in the wurtzite ZnO structure, which retains, however, a high crystalline quality. No segregated secondary phases neither Co-rich nanocrystals were detected. Superconducting quantum interference device magnetometry demonstrates a paramagnetic Curie–Weiss behavior with antiferromagnetic interactions. We discuss the observed room temperature paramagnetism of our samples considering the current models for the magnetic properties of diluted magnetic semiconductors. © *2010 American Institute of Physics*. [doi:10.1063/1.3459885]

## I. INTRODUCTION

Spin injection in semiconductors is a fundamental problem for developing spintronic devices due to the well known impedance mismatch between semiconductors and ferromagnetics.[1] III-V diluted magnetic semiconductors (DMS) [2,3] was then proposed as an alternative system for spintronic devices with the advantage of introducing new functionalities that are difficult to be implemented in metallic structures, such as electrical control of both the coercivity[4] and the Curie temperature.[5] The magnetic properties of III-V DMS are well explained by an indirect exchange mechanism in which the ferromagnetism (FM) between magnetic ions are mediated by free carriers. Unfortunately the relatively low Curie temperatures ($T_C < 180$ K) of III-V DMS are not appropriate for most practical applications. The prediction of a stable long range magnetic ordering at high temperatures for other transition metal (TM) doped semiconductors,[6] specifically for the Mn-doped GaN and ZnO, followed by the observation of room temperature FM (RTFM) has stimulated a large effort on the research of those materials.

In spite of extensive studies, understanding the magnetic properties of TM-doped ZnO systems still remains a controversial issue, mostly due to the low-reproducibility of the results from samples grown by different preparation methods.[7,8] Experimentally, there are conflicting reports pointing that samples grown under similar conditions may present ferromagnetic or paramagnetic behavior at room temperature.[9,10] The RTFM observed for some samples has been attributed to different origins, including the original model based of FM mediated by free carriers or by shallow donor–electrons forming bound polarons,[11] and alternative explanations such as the formation of a magnetic secondary phase[12] and TM-rich nanocrystals.[13] A conclusive analysis on the presence of the microstructures assigned to those alternative explanations of the RTFM is, however, a difficult task that requires additional analysis than standard characterization techniques.[14]

In the present work we report a detailed study of the microstructure and the magnetic properties of $Zn_{1-x}Co_xO$ bulk samples with Co molar concentrations of 4%, 8%, 12%, 15%, and 21% prepared by a standard solid-state reaction method. Magnetic results demonstrated an absence of ferromagnetic order at room temperature in all samples. We performed a detailed microstructural characterization by conjugating several different techniques, in order to understand the origin of the paramagnetic behavior of the samples considering the proposed models for the magnetic properties of TM-doped ZnO.

## II. EXPERIMENT

Polycrystalline $Zn_{1-x}Co_xO$ ($x=0.04$, 0.08, 0.12, 0.15, and 0.21) bulk samples were prepared by the standard solid-state reaction method. Stoichiometric amounts of ZnO (99.998%) and $Co_3O_4$ (99.7%) were mixed and ball milled for 5 h using Zn spheres. The resulting powder was cold compacted by an uniaxial pressure of 600 MPa in the form of

[a)]Electronic mail: bonette@unifal-mg.edu.br.

 

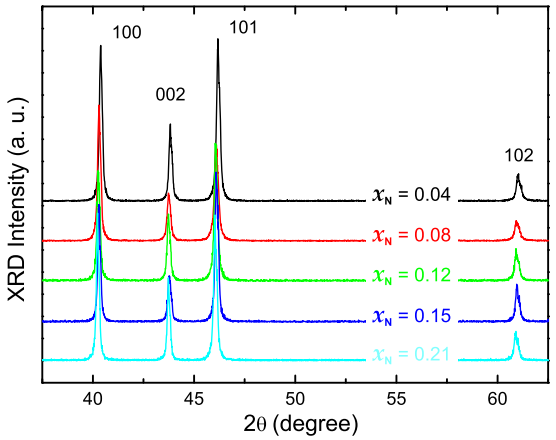


FIG. 1. (Color online) XRD diffratograms of polycrystalline samples. All peaks belong to the hexagonal structure of wurtzite ZnO.

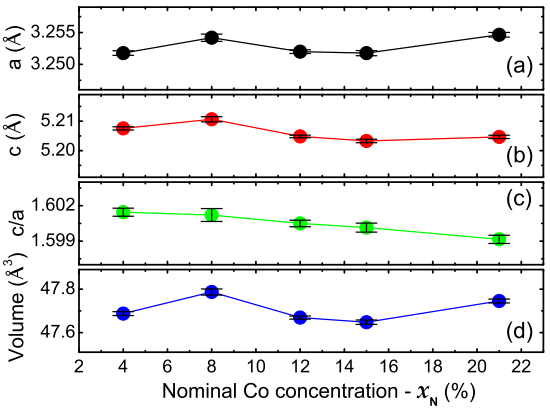


FIG. 2. (Color online) Lattice parameters a (a), c (b) of the wurtzite structure, c/a ratio (c), and unit-cell volume (d) determined from the XRD for $Zn_{1-x}Co_xO$ samples.

pellets (green pellets). The green pellets were finally sintered in oxygen atmosphere at 1400 °C for 4 h. The crystalline structure of the samples was studied using a Philips x-ray diffractometer (XRD) employing Fe $K\alpha$ radiation and a graphite monochromator. XRD data was recorded in the range of $2\theta=35.00°-65.00°$ with steps of 0.01° at 1.2 s/step. Structural analysis was performed using the Rietveld method as implemented by the software package FULLPROF.[15] The microstructure and the composition distribution were also characterized using a scanning electron microscope (SEM) and an energy dispersive x-ray spectrometer (EDS). To determine the valence state of the Co dopant in the ZnO lattice, Co K-edge x-ray absorption near edge structure (XANES) was measured in the transmittance mode at the XAS beamline from the Brazilian Synchrotron Light Laboratory (LNLS), Campinas, Brazil. Raman spectroscopy was used to study the Co incorporation on the ZnO matrix and the resulting lattice disorder as well as to analyze the formation of segregated secondary phases. Raman was carried out at room temperature using a Jobin-Yvon-64000 micro-Raman system in the backscattering geometry using the 488 nm line of an $Ar^+$ laser for excitation. We used an optical objective of 100× magnification, which gives an average laser spot size of 1 $\mu$m. Magnetic measurements were performed using a superconducting quantum interference device magnetometer.

## III. RESULTS AND DISCUSSION

Figure 1 shows the XRD results for the whole set of samples. The observed peaks correspond to those expected for polycrystalline wurtzite ZnO and present relative narrow line-widths. The results reveal a high crystalline quality for all samples. No indication of additional phases were observed within the detection limit of the measurement. The lattice parameters obtained from the XRD measurements are presented in Fig. 2. There is no significant change in the wurtzite cell lattice parameters as the Co concentration is increased. This result indicates that the ionic radii ($r$) of the Co atoms incorporated in the material should be very close to the ionic radii of Zn in the ZnO matrix. For the ZnO wurtzite structure, the Zn is tetrahedrally coordinated with valence 2+ and $r=0.60$ Å. The closest ionic radii assumed by Co is when it is also tetrahedrally coordinated with valence 2+ ($r=0.58$ Å).[16] Therefore, our results indicates that Co replaces Zn ions in the ZnO matrix with a 2+ valence.

Figure 3 shows representative SEM images of our samples that reveal intergrannular fractured surfaces. A series of full scans over large areas confirm the absence of Co-rich nanoclusters. Furthemore, SEM results show no evidence of secondary phases in our samples. The effective Co concentrations of the $Zn_{1-x}Co_xO$ samples ($x_E$) were also measured by EDS analysis and are presented in Fig. 3(f) as a function of the nominal Co concentration ($x_N$). We observe a good agreement between the measured and the nominal concentration values.

XANES spectra give information on the coordination symmetry and the valence of ions incorporated in a solid.

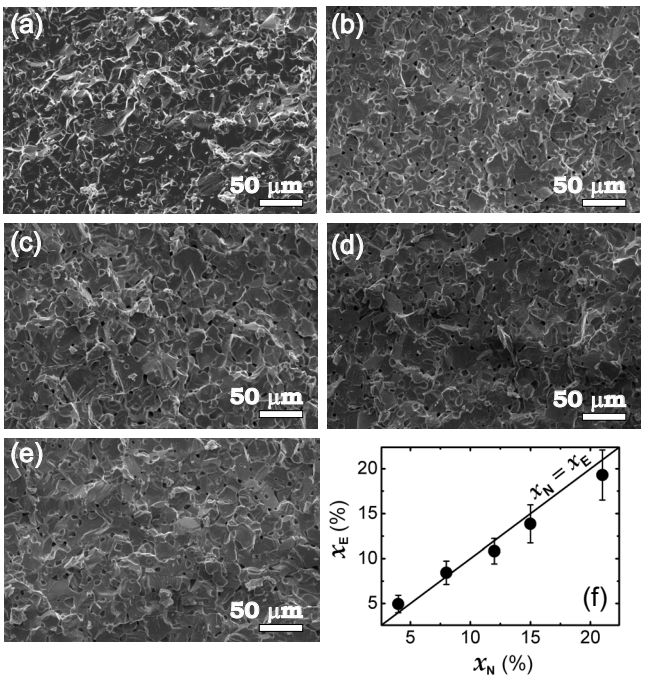


FIG. 3. Representative scanning electron micrographs of $Zn_{1-x}Co_xO$ samples with (a) $x=0.04$, (b) 0.08, (c) 0.12, (d) 0.15, and (e) 0.21 (mag.: 350×). (f) Effective Co concentrations obtained from EDS ($x_E$) vs nominal concentration ($x_N$).

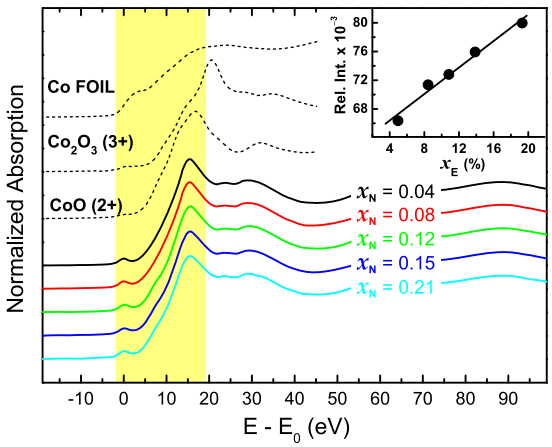


FIG. 4. (Color online) Experimental Co K-edge XANES spectra for the five $Zn_{1-x}Co_xO$ samples ($E_0$=7708.8 eV). Spectra of metallic Co, rocksalt CoO (valence 2+) and $Co_2O_3$ (valence 3+) are also shown for comparison. The inset shows the relative intensity of pre-edge peak as a function of effective Co concentration.

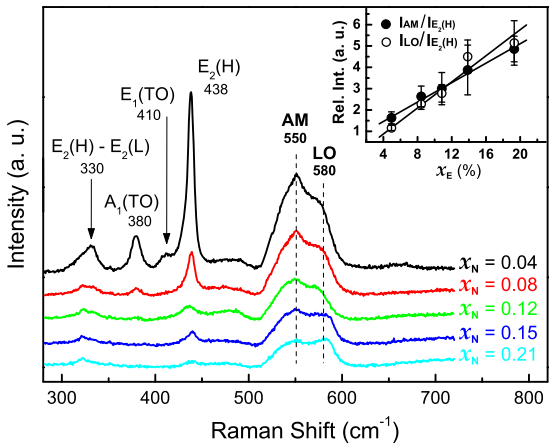


FIG. 5. (Color online) Raman scattering spectra of $Zn_{1-x}Co_xO$ samples at room temperature. The inset presents the relative intensity of the LO and AM modes as a function of effective Co concentration (the intensities were obtained from multipeak Lorentz fittings).

The energy of the absorption edge shifts according to the valence of the absorbing ion, since the binding energy of bound electrons rises as the valence increases. Also, the shape of the absorption edge depends on the unfilled local density of states and the coordination symmetry of the absorbing element. Figure 4 shows the XANES spectra obtained for our $Zn_{1-x}Co_xO$ samples at room temperature. All spectra have similar features, except by small differences on the relative peak intensities at the pre-edge regions. This is an indication that there is no significant structural distortion around the Co ions for different doping levels. Generally, the intensity of the pre-edge peak increases linearly with the substitutional incorporation of a TM in a solid due to a progressive participation of the 3*d* orbital in the bonding.[17] The inset of Fig. 4 presents in fact the linear evolution of the intensity of the pre-edge peak relative to the white line maximum. The valence of the dopant ions can be analyzed by comparing their resulting edge structure from those obtained from reference samples. In Fig. 4 we also present XANES spectra from Co ions from oxides with various metal oxidation states. The comparison with the spectra from our samples indicate that Co assumes predominantly the 2+ oxidation state, which corroborates the XRD results.

Raman spectra from our set of samples are shown in Fig. 5. The $Zn_{1-x}Co_xO$ samples, as well as ZnO, presents the wurtzite structure for small Co compositions.[18] In this case, only the $A_1$, $E_1$, and $E_2$ modes are Raman active,[19] where the $A_1$ and $E_1$ are optical phonon modes [transversal optical and longitudinal optical (LO)] and the $E_2$ is a nonpolar mode. The frequency of ZnO modes are well established in the literature.[19,20] We observe a series of narrow peaks centered at 330, 380, 410, and 438 $cm^{-1}$, that are assigned to the $E_2(H)-E_2(L)$, $A_1(TO)$, $E_1(TO)$, and $E_2(H)$ ZnO modes, respectively. The peaks are observed for all samples but they are better defined for the sample with the lowest Co content ($x$=0.04). We also observe a broad band at $\sim$500–600 $cm^{-1}$. The broad band seems to enclose several peaks, whereas the main ones are centered at $\sim$550 and 580 $cm^{-1}$.The peak at $\sim$580 $cm^{-1}$ can be attributed to the overlap of the LO phonons of the $A_1$ and $E_1$ modes[19] but the peak at $\sim$550 $cm^{-1}$ cannot be attributed to a ZnO mode; it is indexed as an additional mode (AM). In pure ZnO, the $A_1$(LO) and $E_1$(LO) modes are usually very weak due to the destructive interference between the deformation and the Frölich potentials.[21] Nevertheless, crystalline disorder due to impurities or defects can result in the amplification of those modes due to the breaking out of the k-conservation law, giving rise to a broad band that reflects the density of phonon states around those frequencies, as observed for Ga implanted ZnO.[22] In our samples, Co atoms are also expected to introduce disorder in the crystal, which can explain the emergence of the broad band. For the sample with $x$=0.04, the $E_2$(H) peak is dominant, but as the Co composition increases, the broad band becomes the dominant feature of the Raman spectra, the inset of Fig. 5 shows that the relative intensity of LO and AM mode with respect to the $E_2$(H) intensity increases almost linearly with effective Co concentration. Similar features around 500–600 $cm^{-1}$ were observed in several works on TM,[18,23–25] Ce,[26] and Sb-doped ZnO samples.[27] In those works the main peak of the broad band is, however, at $\sim$530 $cm^{-1}$, and it has been attributed to complexes involving intrinsic defects, such as oxygen vacancies ($V_O$) and Zn interstitials ($Zn_i$). Based on correlations between different samples procedures and their magnetic properties it has been proposed that this peak is related to the origin of RTFM on ZnO.[28] Recently, theoretical calculations have been presented supporting that the RTFM on Co-doped ZnO systems can be a critical combination of doping and broadening of Co-related states due to the presence of intrinsic defects, resulting in an increase in the carrier-mediated interaction between magnetic ions.[29]

A significant result from the Raman data is the complete absence of peaks related to segregated secondary phases, as it has been observed for some Co-doped ZnO samples. The most common secondary phases are CoO and $Co_3O_4$.[30,31] CoO presents two sharp lines at 484 (weak) and 691 (strong) $cm^{-1}$ associated to the $A_g$ and $E_g$ modes and a broad band between 500 to 600 $cm^{-1}$ attributed to anharmonic interactions.[32] $Co_3O_4$ present five sharp lines at 197

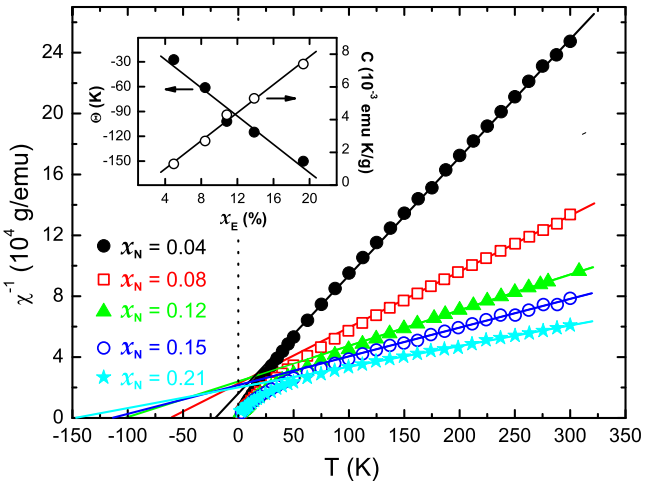


FIG. 6. (Color online) Inverse susceptibility vs. temperature for $Zn_{1-x}Co_xO$ samples. The best fit of the high temperature data to Curie–Weiss law is shown as solid lines. The inset shows Θ (full symbols) and $C$ (open symbols) as a function of $x_E$, solid lines are linear fit to the data.

($F_{2g}$), 485 ($E_g$), 523 ($F_{2g}$), 624 ($F_{2g}$), and 693 ($A_{1g}$).[32] For both materials the peak at ~690 $cm^{-1}$ is always the strongest one. We do not observe, however, any indication of a peak at this frequency for our set of samples. Therefore, Raman scattering results corroborates with the x-ray diffraction results, as it indicates that secondary phase segregation is absent in our samples.

We now proceed with the magnetic characterization. The inverse of the magnetic susceptibility as a function of the temperature is presented in Fig. 6 for our set of samples. The diamagnetic background of the ZnO matrix ($-0.33 \times 10^{-6}$ emu/g) was determined by measuring an undoped ZnO sample used as a reference and then subtracting this value from the raw data. The results show a clear linear behavior for high temperatures. At this range, the magnetic susceptibility can be described using the paramagnetic Curie–Weiss equation

$$\chi = \frac{C(x)}{T - \Theta(x)}, \tag{1}$$

where both the Curie–Weiss temperature, Θ, and the Curie constant per gram, $C$, should present a linear dependence on the TM concentration $x$: $\Theta = \Theta_0 \cdot x$ and $C = C_0 \cdot x$. The constants $C_0$ and $\Theta_0$ are defined as

$$C_0 = \frac{N g_{\text{eff}}^2 \mu_B^2 S(S+1)}{3k_B} \tag{2}$$

and

$$\Theta_0 = \frac{2zS(S+1)J_1}{3k_B}, \tag{3}$$

where $N$ is the number of cations per gram, $g_{\text{eff}}$ is the effective gyromagnetic factor of the Co ion, $S = 3/2$ is the spin for $Co^{2+}$, $\mu_B$ is the Bohr magneton, $z$ is the number of nearest neighbors ($z = 12$ in the wurtzite structure), $J_1$ is the effective exchange integral constant, and $k_B$ is the Boltzmann constant. The values of Θ and $C$ obtained by fitting the results from Fig. 6 using Eq. (1) are presented in the inset of Fig. 6 as a function of the effective Co concentration. All samples present negatives Θ, indicating an antiferromagnetic interaction between Co ions. We can also determine the parameters $C_0$ and $\Theta_0$ by fitting the results presented in the inset of Fig. 6. Finally, using the known values for the other constants involved in $C_0$ and $\Theta_0$ in the Eqs. (2) and (3), we can estimate the two main magnetic parameters for $Co^{2+}$: $g_{\text{eff}} = 2.72$ and $J_1/k_B = -28.5 \pm 3.6$ K. These values are in good agreement with other results obtained for $Co^{2+}$ in ZnO matrix[30,33] and for other Co-doped II-VI semiconductor.[34]

The observed absence of magnetic order in our samples is consistent with the absence of the main structures attributed to RTFM: Co-rich nanocrystals, segregated secondary magnetic phases and the specific defect related to the origin of the Raman band at ~530 $cm^{-1}$. Even though our samples present some concentration of defects, as demonstrated by the emergence of the Raman band at ~500–600 $cm^{-1}$, they are not efficient on enhancing the interaction between Co atoms, and therefore, do not promote RTFM.

## IV. CONCLUSION

In summary, we have presented a complete microstructure and magnetic analysis of bulk $Zn_{1-x}Co_xO$ samples prepared through solid-state reaction method. Microstructure results confirm that Co ions substitute Zn ions in the wurtzite ZnO structure with a valence 2+. There is no indication of Co-rich nanoclusters or segregated secondary phases in the samples. Magnetization measurements reveal a Curie–Weiss behavior of the susceptibility at high temperatures characterized by the antiferromagnetic interaction between Co ions. Our results demonstrate that the substitution of Zn by the Co dopant in the wurtzite ZnO structure is not a sufficient condition to achieve RTFM, which seems to be critically dependent on the presence of some specific defects that alter the carrier distribution and affect the carrier-mediated interaction between the magnetic ions.

## ACKNOWLEDGMENTS

Support from agencies FAPEMIG, CNPq and FAPESP are gratefully acknowledged. The authors also acknowledge LNLS for the XANES measurements and Professor Dr. G. M. da Costa of the Universidade Federal de Ouro Preto for the XRD measurements.

[1] G. Schmidt, D. Ferrand, L. W. Molenkamp, A. T. Filip, and B. J. van Wees, Phys. Rev. B **62**, R4790 (2000).
[2] R. Fiederling, M. Keim, G. Reuscher, W. Ossau, G. Schmidt, A. Waag, and L. W. Molenkamp, Nature **402**, 787 (1999).
[3] Y. Ohno, D. K. Young, B. Beschoten, F. Matsukura, H. Ohno, and D. D. Awschalom, Nature **402**, 790 (1999).
[4] D. Chiba, M. Yamanouchi, F. Matsukura, and H. Ohno, Science **301**, 943 (2003).
[5] H. Ohno, D. Chiba, F. Matsukura, T. Omiya, E. Abe, T. Dietl, Y. Ohno, and K. Ohtani, Nature **408**, 944 (2000).
[6] T. Dietl, H. Hono, F. Matsukura, J. Cibert, and D. Ferrand, Science **287**, 1019 (2000).
[7] C. Liu, F. Yun, and H. Morkoç, J. Mater. Sci.: Mater. Electron. **16**, 555 (2005).
[8] F. Pan, C. Song, X. Liu, Y. Yang, and F. Zeng, Mater. Sci. Eng. R. **62**, 1 (2008).
[9] P. Sharma, A. Gupta, K. Rao, F. J. Owes, R. Sharma, R. Ahuja, J. M. O. Guillen, B. Johansson, and G. A. Gehring, Nature Mater. **2**, 673 (2003).

[10]G. Lawes, A. S. Risbud, A. P. Ramirez, and R. Seshadri, Phys. Rev. B **71**, 045201 (2005).
[11]J. M. D. Coey, M. Venkatesan, and C. B. Fitzgerald, Nature Mater. **4**, 173 (2005).
[12]D. C. Kundaliya, S. B. Ogale, S. E. Lofland, S. Dhar, C. J. Metting, S. R. Shinde, Z. Ma, B. Varughese, K. Ramanujachary, L. Salamanca-Riba, and T. Venkatesan, Nature Mater. **3**, 709 (2004).
[13]T. Dietl, T. Andrearczyk, A. Lipinska, M. Kiecana, M. Tay, and Y. Wu, Phys. Rev. B **76**, 155312 (2007).
[14]R. Seshadri, Curr. Opin. Solid State Mater. Sci. **9**, 1 (2005).
[15]J. Rodriguez-Carvajal, Physica B **192**, 55 (1993).
[16]R. D. Shannon, Acta Crystallogr., Sect. A: Cryst. Phys., Diffr., Theor. Gen. Crystallogr. **A32**, 751 (1976).
[17]W. F. Pong, R. A. Mayanovic, K. T. Wu, P. K. Tseng, B. A. Bunker, A. Hiraya, and M. Watanabe, Phys. Rev. B **50**, 7371 (1994).
[18]T.-L. Phan, R. Vincent, D. Cherns, N. H. Dan, and S.-C. Yu, Appl. Phys. Lett. **93**, 082110 (2008).
[19]T. C. Damen, S. P. S. Porto, and B. Tell, Phys. Rev. **142**, 570 (1966).
[20]R. Cuscó, E. Alarcón-Lladó, J. Ibáñez, L. Artús, J. Jiménez, B. Wang, and M. J. Callahan, Phys. Rev. B **75**, 165202 (2007).
[21]R. H. Callender, S. S. Sussman, M. Selders, and R. K. Chang, Phys. Rev. B **7**, 3788 (1973).
[22]F. Reuss, C. Kirchner, T. Gruber, R. Kling, S. Maschek, W. Limmer, A. Waag, and P. Ziemann, J. Appl. Phys. **95**, 3385 (2004).
[23]X. Wang, J. Xu, X. Yu, K. Xue, J. Yu, and X. Zhao, Appl. Phys. Lett. **91**, 031908 (2007).
[24]J. B. Wang, G. J. Huang, X. L. Zhong, L. Z. Sun, Y. C. Zhou, and E. H. Liu, Appl. Phys. Lett. **88**, 252502 (2006).
[25]Z. Wang, D. Geng, W. Hu, and Z. Zhang, J. Appl. Phys. **105**, 123902 (2009).
[26]B. Cheng, Y. Xiao, G. Wu, and L. Zhang, Appl. Phys. Lett. **84**, 416 (2004).
[27]C. Bundesmann, N. Ashkenov, M. Schubert, D. Spemann, T. Butz, E. M. Kaidashev, M. Lorenz, and M. Grundmann, Appl. Phys. Lett. **83**, 1974 (2003).
[28]V. K. Sharma and G. D. Varma, J. Appl. Phys. **102**, 056105 (2007).
[29]E.-Z. Liu, Y. He, and J. Z. Jiang, Appl. Phys. Lett. **93**, 132506 (2008).
[30]S. Kolesnik, B. Dabrowski, and J. Mais, J. Appl. Phys. **95**, 2582 (2004).
[31]A. Quesada, M. A. García, M. Andrés, A. Hernando, J. F. Fernández, A. C. Caballero, M. S. Martín-González, and F. Briones, J. Appl. Phys. **100**, 113909 (2006).
[32]D. Gallant, M. Pezolet, and S. Simard, J. Phys. Chem. B **110**, 6871 (2006).
[33]S.-J. Han, B. Lee, J.-S. Ku, Y. Kim, and Y. Jeong, J. Magn. Magn. Mater. **272**, 2008 (2004).
[34]H. Alawadhi, I. Miotkowski, A. Lewicki, A. K. Ramdas, S. Miotkowska, and M. McElfresh, J. Phys.: Condens. Matter **14**, 4611 (2002).